Available online at www.sciencedirect.com
ScienceDirect
Journal of Catalysis 244 (2006) 183–191
JOURNAL OF CATALYSIS
www.elsevier.com/locate/jcat

An investigation of possible mechanisms for the water–gas shift reaction over a ZrO_2-supported Pt catalyst

D. Tibiletti [a], F.C. Meunier [a,*], A. Goguet [a], D. Reid [a], R. Burch [a], M. Boaro [b], M. Vicario [b], A. Trovarelli [b]

[a] *CenTACat, School of Chemistry and Chemical Engineering, Queen's University Belfast, Belfast, BT9 5AG, Northern Ireland*
[b] *Dipartimento di Scienze e Tecnologie Chimiche, Università di Udine, 33100 Udine, Italy*

Received 18 July 2006; revised 31 August 2006; accepted 5 September 2006

Available online 10 October 2006

Abstract

The present work investigates the reactivity of the surface species observable by in situ DRIFTS formed over a Pt/ZrO_2 during the water–gas shift (WGS) reaction. A DRIFTS cell/mass spectrometer system was operated at the chemical steady state during isotopic transients to yield information about the true nature (i.e., main reaction intermediate or spectators) of adsorbates. Only carbonyl and formate species were observed by DRIFTS under reaction conditions; the surface coverage of carbonate species was negligible. Isotopic transient kinetic analyses revealed that formates exchanged uniformly according to a first-order law, suggesting that most formates observed by DRIFTS were of the same reactivity. In addition, the time scale of the exchange of the reaction product CO_2 was significantly shorter than that of the surface formates. Therefore, a formate route based on the formates as detected by DRIFTS can be ruled out as the main reaction pathway in the present case. The number of precursors of the reaction product CO_2 was smaller than the number of surface Pt atoms, suggesting that carbonyl species or some "infrared-invisible" complex (not excluding formates) at the Pt–zirconia interface was the main reaction intermediate. A simple redox mechanism could also explain the present results.

Keywords: Formate; DRIFT; FTIR; Operando; In situ; Spectroscopy; Water–gas shift; Reaction intermediate; Spectator; SSITKA; Platinum; Zirconia

1. Introduction

The water–gas shift (WGS) reaction and the corresponding low- and high-temperature catalysts (i.e., Cu and hematite-based formulations, respectively) are well-established features of large-scale industrial production of hydrogen [1,2]. Yet, the interest in novel low-temperature WGS catalysts has been growing steadily in relation to fuel cell technology [3–5]. The need to develop fuel cell processors capable of more efficiently converting fuels into high-purity hydrogen has led to intensive research into developing new catalytic formulations able to satisfy the necessary criteria for this application, that is, (i) high activity in the temperature range 473–553 K, (ii) no need for activation before use, (iii) resistance to poisoning under a reformer atmosphere, and (iv) no degradation on exposure to air or temperature cycles. Formulations based on noble metals (NM), such as Pt and Au on reducible supports, have been recently proposed [3,6–8]. Pt-supported on zirconia [9,10] or mixed-oxide ceria–zirconia [11,12] have been of particular interest.

Although numerous mechanistic and kinetics studies have been carried out in recent years, disagreement remains about the nature of the reaction intermediates and the active sites of NM supported on redox oxides. Two reaction mechanisms are mainly proposed in the literature: the "adsorptive mechanism" (involving in particular formate surface species) and the "regenerative mechanism" (redox). In the regenerative mechanism [13–20], water adsorbs and dissociates on a partly reduced support, releasing H_2 and reoxidising ceria. In parallel, $CO_{(g)}$ adsorbs on metallic sites to form a NM-bound carbonyl species, which then reduces the support and releases CO_2. This model is consistent with that proposed by Grenoble and Estadt [21], who

* Corresponding author. Fax: +44 28 90 382117.
E-mail addresses: f.meunier@qub.ac.uk (F.C. Meunier), marta.boaro@uniud.it (M. Boaro).

0021-9517/$ – see front matter
doi:10.1016/j.jcat.2006.09.004

studied the effect of various supports on the reaction rate and concluded that the WGS reaction occurred through a bifunctional mechanism; the metal activated the carbon monoxide, and support sites were the principal sites for water activation. Various authors have also reported a relationship between catalyst activity and the redox properties of the support [22–24].

In the adsorptive (or associative) mechanism [25–30], CO and H_2O are proposed to adsorb on the catalyst and form a surface intermediate, which subsequently decomposes as H_2 and CO_2. Many research groups have tried to identify the nature of the main intermediate species mainly by isotopic labelling experiments and FT-IR spectroscopy. Formate species have been proposed for the forward-WGS reaction [25,31–33] and carbonates for both the forward [34] and reverse-WGS reaction [35]. In work published by Jacobs et al. [12], it has been proposed that one of the metal's main roles would be to favour the formation of reactive surface hydroxyl groups (type-II) on the oxide support, which would lead to increased formation of formate species.

Our laboratory has recently shown that the reactivity of formates and other surface species formed over Pt/CeO_2 catalyst under reverse was–gas shift (RWGS) feed conditions was strongly dependent on the experimental procedure used, stressing the need to use steady-state and *operando* methods [36]. The formate species, monitored by *operando* DRIFTS combined with the utilisation of isotopic tracer methods (i.e., SSITKA), appeared to undergo isotopic exchange slower than the formation of the reaction product (i.e., ^{13}CO) under steady-state conditions, indicating that these species were not "main" reaction intermediates. It was proposed that formates were therefore "minor" reaction intermediates, meaning that these species are associated with a reaction pathway that may lead to the reaction product. But that would account for only a minor fraction of the actual product yield. Importantly, our work indicated that two or more reaction pathways may occur simultaneously over Pt/CeO_2.

Gong et al. [37] studied the WGS reaction using density functional theory (DFT). In the redox mechanism, the highest energetic barrier is ca. 0.9 eV, corresponding to the hydroxyl decomposition $OH \rightarrow O + H$. The highest energetic barrier in the adsorptive mechanism is the formate decomposition, $HCOO \rightarrow CO_2 + H$, at 1.02 eV. If there were an OH group on the surface near the surface HCOO, then the hydrogen on the surface formate could pass to the hydroxyl, leading to CO_2 and H_2 with an even lower barrier. However, the authors concluded that both mechanisms were possible and that surface coverage could play an important role in determining the reaction pathway. In this regard, Farrauto et al. [38] and Meunier et al. [39] recently proposed that surface carbonates are a potential main reaction intermediate that normally readily decomposes to $CO_{2(g)}$, but that overreduction of the CeO_2 support could lead to a strengthening of the carbonate bonds, resulting in self-poisoning of the catalyst by one of the reaction products [40].

Noble metals solely supported on either ZrO_2 or CeO_2 are typically less active than the corresponding mixed oxide-based materials, but it is important and enlightening to investigate the individual components. We also must point out that the reactivity of ZrO_2- and CeO_2-based materials strongly depends on their method of preparation. As an example, some of us have recently shown that the activity in CO oxidation on similarly prepared ceria powders is strongly dependent on type of surface planes exposed [41]. These in turn are modified by thermal treatments. Moreover, it must be stressed that ZrO_2 alone is present in different polymorphs (tetragonal and monoclinic) that exhibit different structural and acid–base surface properties; therefore, the similarities between ZrO_2 and CeO_2 are not always obvious [42].

In contrast to some other catalysts, for which complications due to the influence of an easily reducible support (e.g., CeO_2 or Fe_2O_3) can make it difficult to define a unique mechanism for the WGS reaction, plain ZrO_2 is less readily reduced (see the TPR data in Ref. [9]); thus, it may be possible to better differentiate between processes on the metal or at the metal–support interface and those occurring across the support. In the present work, the nature and reactivity of the surface species formed under *operando* conditions during the WGS reaction over Pt supported on ZrO_2 is presented and the role of formate species is discussed.

Based on a DRIFT + MS/SSITKA technique [39,43,44], the data reported here unambiguously show that the route based on the formate observed by DRIFTS is only a "minor" reaction pathway under the present experimental conditions used for our Pt/ZrO_2. This stresses that another route, the details of which are yet unclear but could possibly be related to a redox-type mechanism, must be present and accounts for most of the sample activity under the present conditions. Although plain ZrO_2 can be difficult to reduce even at high temperatures (e.g., not below 800 °C [9]), various groups have reported temperature-programmed reaction studies clearly showing that Pt-promoted zirconia was starting to reduce below 200 °C [9,12], and thus a redox mechanism is possible, at least at the metal–support interface, under the conditions reported here.

2. Experimental

2.1. Sample preparation

The support used was a commercial ZrO_2 supplied by Magnesium Elektron Limited, calcined at 923 K. The platinum was deposited by incipient wetness impregnation of $H_2PtCl_6{\cdot}6H_2O$ (Aldrich). The support was first dried and then impregnated with an appropriate volume of the aqueous solution of Pt precursor, corresponding to the support pore volume. The solution was added dropwise, stirring the catalyst precursor until pore saturation. To achieve the desired loading, the impregnation was repeated three times. The sample was dried at 383 K overnight, crushed, and calcined at 823 K in a tubular reactor for 1 h in air (200 $cm^3\,min^{-1}$), using a temperature ramp of 10 $K\,min^{-1}$.

2.2. Sample characterization

The specific surface area was measured by the BET method on a Tristar 3000 (Micrometrics) gas adsorption analyser. X-ray

powder diffraction patterns were collected using a Philips PW3040/60 X'pert PRO instrument (equipped with an X'celerator detector) operated at 40 kV and 40 mA, with an Ni-filtered Cu$K\alpha$ radiation source. The diffractograms were collected with a step size of 0.02° and a counting time of 40 s per angular abscissa in the range of 20°–145°.

The Pt dispersion was estimated using H_2 chemisorption analysis, carried out on a Micromeritics ASAP 2000 analyser. The H_2 chemisorption experiments were conducted at 183 K on 0.2 g of catalyst. The calcined sample was subjected to a standard cleaning procedure consisting of heating the sample under O_2 (5%)/Ar at 773 K for 1 h. The samples were then prereduced in a flow of H_2 (35 ml min^{-1}) at 473 K. After 2 h at this temperature, the samples were evacuated at 673 K for 4 h and cooled under vacuum to the adsorption temperature (183 K). Typically, an equilibration time of 10 min was used. Adsorbed volumes were determined by extrapolation to zero pressure of the linear part of the adsorption isotherm (100–400 Torr) after elimination of the so-called "reversible hydrogen adsorption." A stoichiometry of 1:1 between the surface Pt site and hydrogen atom was assumed.

2.3. In situ DRIFTS studies and SSITKA–DRIFTS/MS experiments

The in situ DRIFTS experiments were carried out as described previously [40]. In brief, it consisted of an in situ high-temperature diffuse reflectance IR cell (Spectra-Tech) fitted with ZnSe windows. The crucible was modified to ensure essentially plug-flow conditions through the catalyst bed. The interface between the ceramic reactor and the metallic base plate was sealed with PTFE tape to prevent any sample bypass [39]. The cell was connected to the feed gas cylinders through low-volume stainless steel lines. The purity of the gases used (i.e., H_2, CO and Ar, supplied by BOC) was >99.95%. The ^{13}CO was 99% pure (supplied by Cambridge Isotope Laboratories). The gas flows were controlled by Aera mass flow controllers, which were calibrated regularly. The water was supplied by bubbling Ar through a metallic water saturator, the temperature of which was controlled by an Eurotherm 2416 controller. A four-way valve was used to allow rapid switching between two reaction feeds, when appropriate. The DRIFTS cell was located in a Bruker Equinox 55 spectrometer, operating at a resolution of 4 cm^{-1}. The outlet of the DRIFTS cell was connected to a quadrupolar mass spectrometer (Hiden HPR20). The mass spectrometer was equipped with a capillary inlet system with bypass allowing fast response (i.e., 100 ms) for the sampling. Both feed lines were connected to an ultra-low differential pressure transducer (Honeywell 395–257) and a high-precision metering valve (Nupro) to equalise the corresponding pressure drops. No variation in the concentration of water was observed on switching between feeds.

The catalyst loaded in the reactor had a particle diameter <150 μm. Before any measurement, the sample was reduced in situ for 30 min at 453 K in a 5% H_2/Ar mixture at a total flow of 100 cm^3 min^{-1}. After the reduction step, the cell was purged with Ar, and the temperature of the reactor was set to achieve ca. 12% conversion. The reaction mixture (i.e., 2% CO, 7% H_2O, 12% H_2 in Ar) was introduced at a total flow rate of 100 cm^3 min^{-1}. The steady-state conditions, as far as the nature and concentration of surface species measured by DRIFTS are concerned, was reached in less than 30 min. A series of back and forth isotopic switches were carried out to assess the reproducibility and precision of the experiment. No kinetic differences could be observed between the forward and backward switches, and symmetric exchange curves were obtained. It was noticed that any set of ^{12}C or ^{13}C species could be used to discuss the results.

The IR data were reported as $\log 1/R$, with $R = I/I_0$, where R is the sample reflectance, I_0 is the intensity measured on the sample after reduction in hydrogen, and I is the intensity measured under reaction condition. The function $\log 1/R$ gives a better linear representation of the band intensity against sample surface coverage than that given by the Kubelka–Munk function for strongly absorbing media such as our catalyst [45,46].

2.4. Analysis of the isotopic exchange rate of the surface species by IR and rate of formation of the reaction products by MS

A least squares linear regression method was used to quantify the extent of the isotopic exchange of the formate species, using the initial (i.e., all ^{12}C) and final (i.e., all ^{13}C) DRIFTS spectra as references. Two different regions of the spectrum were used to integrate the signal of formate species (vide infra). As far as the mass spectrometric analysis was concerned, the masses 28, 44, 29, 45, and 4 (amu), were followed and the data collection was started at least 10 min before the isotopic switches to observe any possible MS baseline drift. The concentrations of the reactants and products were also determined using an on-line gas chromatograph (Perkin–Elmer Clarus), equipped with a HayeSep Q column and a flame ionization detector fitted with a methanator to allow the accurate and precise quantification of CO and CO_2.

3. Results and discussion

3.1. Catalyst structure

The sample characteristics are gathered in Table 1. Fig. 1 shows the XRD patterns of the support and the platinum-loaded catalyst. In both cases, the ZrO_2 was mainly monoclinic, although a tetragonal phase could also be observed. The diffrac-

Table 1
Structural properties of the samples

Sample name	Pt loading (wt%)	Pt dispersion	Average Pt particle size[a] (nm)	Specific surface area[b] (m^2 g^{-1})	XRD structure[c]	Average pore size (nm)
ZrO_2	–	–	–	38 (923 K)	m and t	11.8
Pt/ZrO_2	4	75%	1.5	35 (523 K)	m and t	10.2

[a] Determined from the dispersion.
[b] In parentheses the temperature of calcination.
[c] m = monoclinic; t = tetragonal.

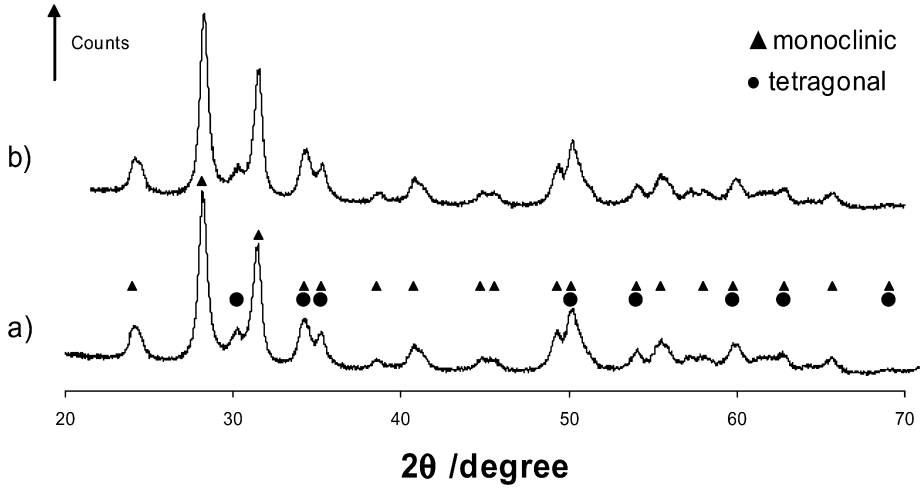

Fig. 1. XRD patterns of (a) ZrO_2, (b) Pt/ZrO_2. In both cases, the patterns corresponded to 90% of the monoclinic polymorph (JCPDS 861450) and 10% of the tetragonal polymorph (JCPDS 79-1770).

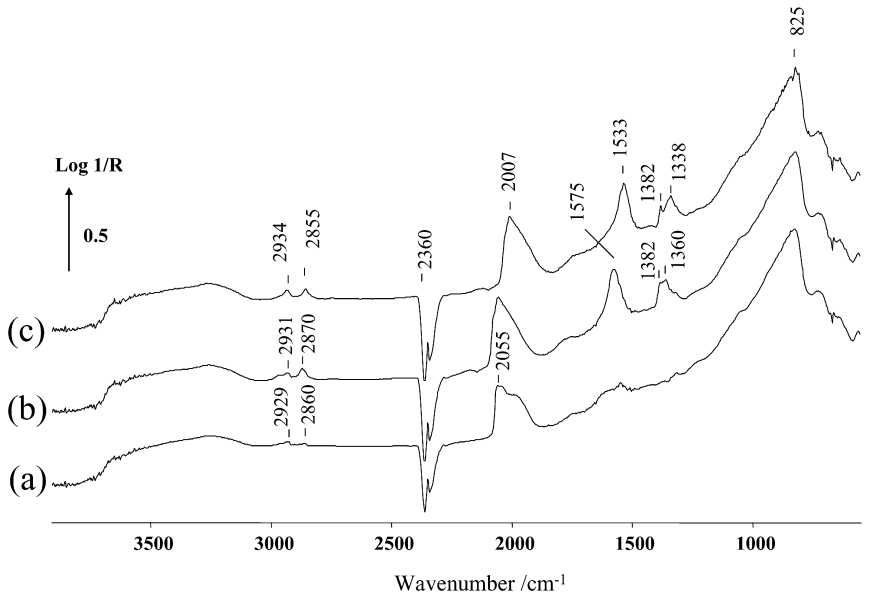

Fig. 2. In situ DRIFT spectra of the Pt/ZrO_2 at 473 K in (a) Ar after prereduction and (b) exposed to the WGS mixture (i.e., 2% ^{12}CO, 7% H_2O, 12% H_2 in Ar) and (c) exposed to the corresponding labelled feed (i.e., 2% ^{13}CO, 7% H_2O, 12% H_2 in Ar). The absorbance with respect to a mirror signal is reported.

tion patterns of the Pt-containing catalysts did not show any peak related to the metal or metal oxide phases, indicating that high dispersion was obtained and the Pt crystallite size was on the order of nanometers. Furthermore, there was no evidence of solid solution formation between Pt and the support; no shift of the support peak was observed. After calcination at 923 K for 2 h, the ZrO_2 specific surface area was equal to 38 $m^2\,g^{-1}$, whereas that of the Pt sample was 35 $m^2\,g^{-1}$. The samples exhibited type IV adsorption isotherms (data not shown), with an average pore size of 10 nm.

3.2. In situ DRIFTS data

The DRIFTS spectra of the Pt catalyst at 473 K after prereduction under Ar and under the WGS mixtures (i.e., 2% CO, 7% H_2O, 12% H_2 in Ar, and the corresponding ^{13}C-labelled feed) are shown in Fig. 2. The absorbance with respect to the signal obtained using a mirror in place of the sample is reported. In all cases, the large band observed at around 825 cm^{-1} was associated with zirconia phonon modes, and the broad and ill-defined band observed between 3700 and 3000 cm^{-1} was due to H-bonded hydroxyl groups [47]. Note that the negative band at 2360 cm^{-1} was due mostly to ambient CO_2 signal variations and is of no significance here.

A series of bands around 2055 cm^{-1} was observed in both the sample under Ar (Fig. 2a) and that under the ^{12}C-containing WGS feed (Fig. 2b). These bands are unambiguously assigned to Pt-bound carbonyl species [48]. The fact that such species were present over the sample not yet exposed to the WGS feed can be simply reconciled by the fact that some C-containing species, such as carbonates, were reduced during the pretreatment yielding CO, which then adsorbed onto the Pt. In a similar

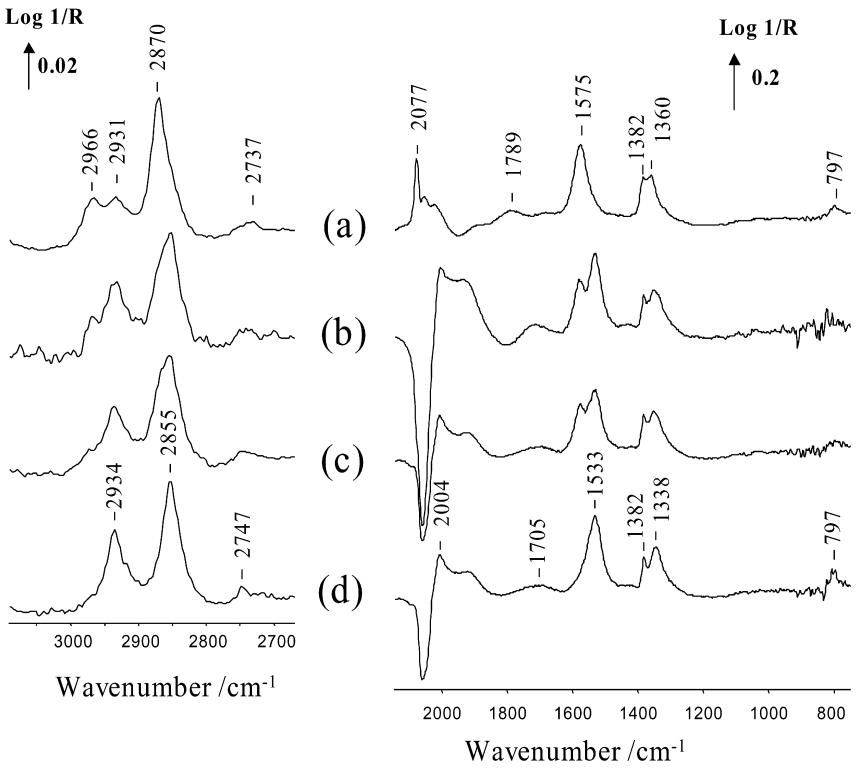

Fig. 3. In situ DRIFT spectrum of the surface species observed over a 4% Pt/ZrO_2 at 473 K at steady state under (a) 2% ^{12}CO, 7% H_2O, 12% H_2 in Ar, and then under 2% ^{13}CO, 7% H_2O, 12% H_2 in Ar for (b) 0.75, (c) 2 and (d) 30 min. The signal of the reduced catalyst at the same temperature under Ar was used as background.

way, ill-defined bands at around 2900 and 1500 cm^{-1} can be observed over the prereduced sample and were mostly formate-type species formed by CO adsorption over the support [49–54].

The corresponding absorbance spectra using the signal obtained over the sample under Ar as reference background are given in Fig. 3. Fig. 3a clearly shows that the surface concentration of ^{12}C-containing formates was markedly increased under the ^{12}CO-containing WGS feed. Most of the clearly observable bands (i.e., 797, 1360, 1382, 1575, 2737, 2870, 2931, and 2966 cm^{-1}) were all associated with surface formate species [47]. The band structure between 3000 and 2700 cm^{-1} is quite complex (Fig. 3a, left), and various assignments have already been discussed by Busca and co-workers [47]. The 2931 cm^{-1} band is actually somewhat reminiscent of a band associated with the ^{13}C-containing species (Fig. 3b), but we can confidently exclude any contamination due to the ^{13}C-containing feed and clearly confirm the earlier assignment by Busca et al. of this particular band to a (^{12}C-containing) formate. Some minor modifications of the carbonyl region (i.e., 2100–1700 cm^{-1}) peak were observed under WGS feed and those could possibly be related to modification of the shape of Pt particles or competitive adsorption phenomena over the Pt surface.

It is noteworthy the absence of any detectable bands in the spectral region at around 860 cm^{-1}, which would be typically associated with the carbonate out-of-plane bending [36]. This stresses that under reaction conditions, the amount of adsorbed carbonate was negligible, as already indicated by the lack of any band other than formates in the 1700–1200 cm^{-1} region, in which OCO stretching modes typically appear.

The details of the spectra obtained under the ^{13}C-containing feed (Fig. 3b) were very similar to those observed under ^{12}C, except for the fact that most bands exhibited a red shift. Note that the band at 797 cm^{-1} (Fig. 3a) was associated with the OCO bending mode of the ^{12}C-formate, which was not expected to shift when exchanging ^{12}C with ^{13}C, as was confirmed here (Fig. 3b). Because no carbonate species were present, either the CH or the OCO stretching region could be used to quantify the relative exchange of the formate species during the SSITKA experiments. These analyses were carried out by using the 3100–2600 cm^{-1} region and the 1667–1411 cm^{-1} region, based on a least squares linear regression method using the initial ^{12}C and final ^{13}C spectra as references. It is interesting to note that the use of either region led to essentially the same transient response (Fig. 4a). This observation emphasised the accuracy and reliability of this analytical method. In addition, the semilogarithmic plot (Fig. 4b) of the same data indicated that the exchange curve of the formates was a single exponential curve, suggesting that the reactivity of all of the formate species as observed by IR was uniform and followed a first-order law.

3.3. MS experiments

The isotopic exchange of the reactant ^{13}CO and that of the reaction product $^{13}CO_2$ were recorded by MS experiments (Fig. 5), simultaneous to the DRIFTS data presented in the pre-

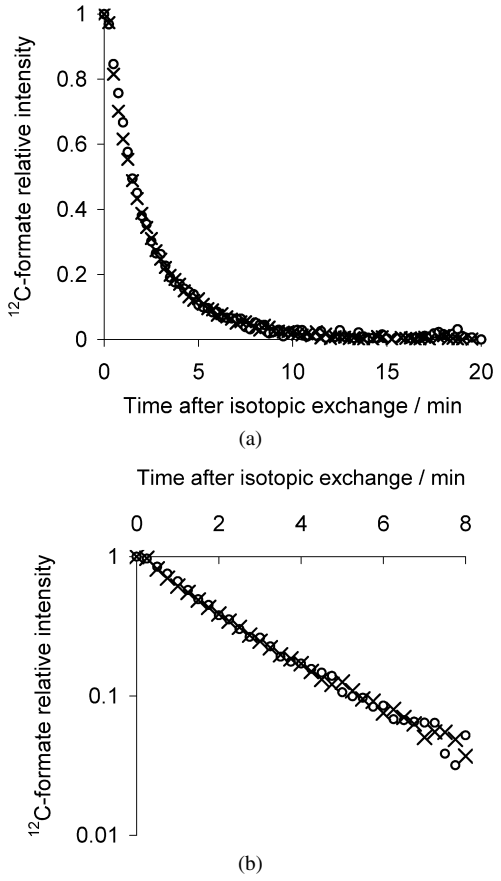

Fig. 4. (a) Comparison of the variation of the DRIFT signal of ^{12}C-formate species during the isotopic exchange evaluated using (○) the CH stretching region around 2860 cm^{-1} and (×) the OCO asymmetric stretch region around 1550 cm^{-1} (see text for integration details). (b) Same as (a), plotted in a semi-logarithmic mode. Feed: 2% ^{13}CO, 7% H_2O, 12% H_2 in Ar, following steady state under 2% ^{12}CO, 7% H_2O, 12% H_2 in Ar. $T = 473$ K.

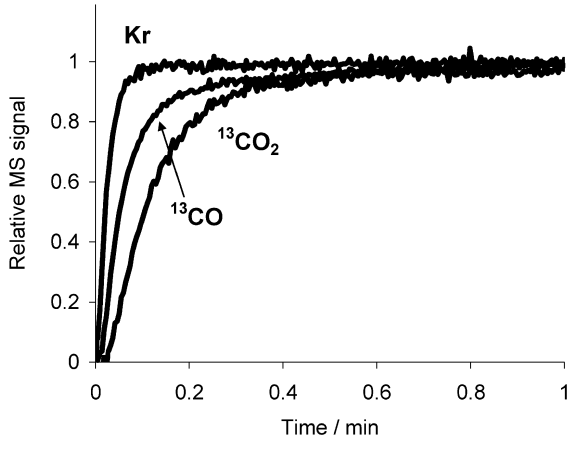

Fig. 5. MS traces of Kr, ^{13}CO and $^{13}CO_2$ for the isotopic switch experiment over the Pt/ZrO_2 catalyst. Feed: 2% ^{13}CO, 7% H_2O, 12% H_2 in Ar, following steady state under 2% ^{12}CO, 7% H_2O, 12% H_2 + 1% Kr in Ar. $T = 473$ K.

vious section. The relative intensity of the MS signal of Kr, used as a tracer, reached steady state in less than 0.1 min (Fig. 5). This value gives an indication of the time resolution of our setup. The exchange of both the reactant and product were essentially complete in less than 0.5 min. The area between the

Table 2
Quantitative data derived from the MS-SSITKA curves

N_{CO}, precursors of $CO_{(g)}$ 10^{18} g_{cat}^{-1}	N_{CO_2}, precursors of $CO_{2(g)}$ 10^{18} g_{cat}^{-1}	N_{Pt}, surface Pt atoms 10^{18} g_{cat}^{-1}	N_O, surface oxide ions 10^{18} g_{cat}^{-1}
52 ± 5	17 ± 2	93 ± 7	520 ± 10

plot of the tracer and that of the ^{13}CO is related (via CO concentration and flow rate) to N_{CO}, that is, the surface precursors of $CO_{(g)}$ [e.g., carbonyl or formate that desorbs as $CO_{(g)}$] [44,55–57]. In a similar manner, the area between the tracer curve and that of the $^{13}CO_2$ leads to the number of surface precursors of CO_2 [e.g., $CO_{2(ads)}$, carbonates, if any, or formates]. These values of precursor amounts, along with the number of surface Pt and O sites, are given in Table 2. The latter set of values was calculated from the Pt dispersion as determined by H_2 chemisorption (assuming H:Pt = 1:1), the surface area of the catalyst, and the average surface density of oxide ions over the zirconia monoclinic surface (ca. 15 O nm^{-2}).

These data highlight two important facts. First, the number of precursors of the reaction product CO_2 (i.e., $N_{CO_2} = 17 \times 10^{18}$ g_{cat}^{-1}) was significantly lower than the number of surface Pt atoms (i.e., $N_{Pt} = 93 \times 10^{18}$ g_{cat}^{-1}). The number of Pt atoms located at the perimeter of the metal particles (assumed to be hemispheres of diameter 1.5 nm) was 33×10^{18} g_{cat}^{-1}. Therefore it is possible that the catalytically active sites were related only to Pt atoms, for example, all Pt sites or even only those located at the metal–oxide interface.

Second, the number of adsorbed species redesorbing as $CO_{(g)}$ (i.e., $N_{CO} = 52 \times 10^{18}$ g_{cat}^{-1}) was smaller than the number of Pt sites minus the number of precursors of CO_2 (i.e., $N_{Pt} - N_{CO_2} = 75 \times 10^{18}$ g_{cat}^{-1}). This makes it possible that all or the main part of the $CO_{(g)}$ precursors originated simply from Pt-bound carbonyls. Some of the $CO_{(g)}$ could have also arisen from the decomposition of the formates located on the ZrO_2. However, this latter route is likely to be minor because the time scales of the CO exchange (ca. 0.2 min) and the formate exchange (5 min) were significantly different.

3.4. Comparison of the DRIFTS and MS data during the SSITKA experiments

The comparison of the DRIFTS ^{13}C-formate and MS $^{13}CO_2$ data during the isotopic exchange (Fig. 6) reveals in an unambiguous manner that these two species were exchanged on a significantly different time scale and thus were unlikely to be related to one another. The formates half-exchanged in about 2 min, whereas the CO_2 half-exchanged in about 0.1 min. It can be seen that 90% of the CO_2 produced was already exchanged after 0.3 min, whereas only 10% of the ^{12}C-formates had been replaced by the ^{13}C counterpart at this point. This observation clearly indicates that the formates seen by DRIFTS are not responsible for the formation of the reaction product CO_2. Because the exchange of formates appeared to be uniform (Fig. 4b), it is unlikely that any significant fraction of the formates observed by DRIFTS reacted faster than the rest of these

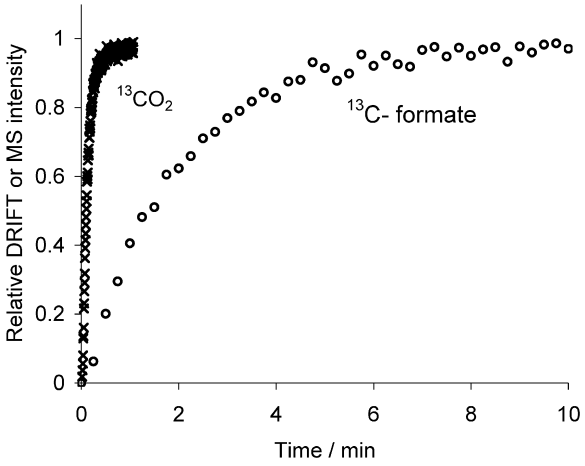

Fig. 6. Normalised MS trace of $^{13}CO_2$ and intensity of the IR band of the ^{13}C-containing formate following the isotopic switch experiments over the Pt/ZrO_2. Feed: 2% ^{13}CO, 7% H_2O, 12% H_2 in Ar, following steady state under 2% ^{12}CO, 7% H_2O, 12% H_2 in Ar. $T = 473$ K.

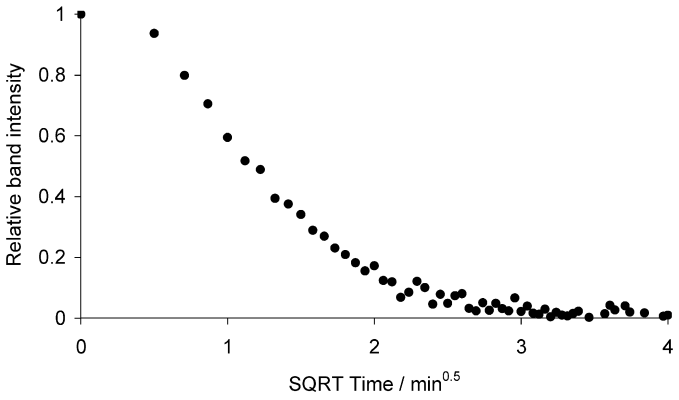

Fig. 7. Variation of the DRIFT signal of ^{12}C-formate species during the isotopic exchange reported as a function of the square root of time. Feed: 2% ^{13}CO, 7% H_2O, 12% H_2 in Ar, following steady state under 2% ^{12}CO, 7% H_2O, 12% H_2 in Ar. $T = 473$ K.

species observed by DRIFTS to account for the formation of CO_2.

The slower exchange of formates compared with that of CO_2 could have been related to the fact that formates reacted to yield CO_2 only at the interface with Pt, as proposed by Davis et al. [58], and thus slow surface diffusion could have limited their rate of exchange. Diffusion on a surface is a two-dimensional phenomenon, and, as in mono-dimensional diffusion, the uptake or exchange of species following a traditional Fickian diffusion model is expected to yield a linear variation of the concentration with the square root of time, up to ca. 50% exchange [59–61]. The plot relating to the formate isotope exchange as a function of the square root of time was not linear (Fig. 7), and thus the surface diffusion of formates to the metal sites was not the limiting step in the process of formate exchange observed here. The data reported in Fig. 4b. actually indicated that the exchange followed a single exponential law, related to a first-order process. In any case, and with involvement of formate diffusion, the misfit between the formate DRIFTS exchange plot and that of the CO_2 (Fig. 6) still indicates that the formates far away from the interface would not significantly contribute to the turnover number.

In addition, the SSITKA data have shown that the number of CO_2 precursors was merely similar to the number of Pt–Zr interface sites, and probably much lower than the number of formates that could bind to oxide sites. (The latter number is not known, but the number of surface oxide ions is 30-times larger than the number of CO_2 precursors; see Table 2.)

One referee suggested that by switching off the water feed (and replacing it by the same flowrate of inert gas), a large increase of the formate concentration would be observed, supporting the presence of highly reactive formate as main reaction intermediates, which would not be observable by IR at steady-state conditions. Although the observation described by the referee may be true, we do not believe that it would constitute unambiguous evidence for the involvement of fast formates, but we cannot reject this argument either. The increased formate concentration could be due simply to modification of the surface structure and/or oxidation state of the catalyst, due to the removal of an oxidiser (i.e., water) while a reducing agent (i.e., CO) was kept in the feed. TPR [9,12] and EPR studies [62,63] support the formation of some reduced centres (i.e., Zr^{3+}) already at the temperature relevant to the present work, these reduced centres having been proposed as the active sites for CO hydrogenation via formate species [64–66]. Bell et al. have also proposed that formation of the anion vacancies may actually facilitate the reaction of CO with neighbouring surface hydroxyl group and lead to surface formate species at temperatures similar to that used here [67,68]. Caution must be observed when using non-steady-state conditions to study the nature and reactivity of surface species over this type of catalyst, even if ZrO_2 is typically less easily reduced than CeO_2, for which the effect of feed composition on the surface reactivity has been clearly demonstrated [40].

Although the present work could not highlight the nature of the main reaction intermediates (e.g., carbonyl or formates located on the Pt or the Pt–ZrO_2 interface), it can be concluded that the "formates observed by IR" located on the ZrO_2 surface were not the main pool of surface compounds leading to CO_2, although those may lead to CO_2 at a much slower rate. These IR-visible formates were minor reaction intermediates and not truly spectator species, because those were eventually exchanged. However, under normal time scales they could not make any significant contribution to the production of CO_2. It would be useful to quantify the exact proportion of CO_2 formed by the IR-observable formates; however, this would require determining the absolute formate surface concentration and the selectivity to which those decompose to either CO or CO_2, which are not straightforward measurements.

As far as the main reaction pathway is concerned, the only IR-observable species that seemed to have a kinetic response comparable to the rate of formation of carbon dioxide is the carbonyl species. It is however impossible to accurately quantify the carbonyl exchange; see the discussion section on carbonyls in [46]. However, the number of CO_2 precursors is lower than the number of surface platinum atoms, assuming that one CO adsorbed per surface Pt atom. This leads us to suggest that on

a support such as zirconia, which is yet difficult to reduce, the WGS mechanism could involve a simple redox mechanism as described by Flytzani–Stephanopoulos et al. and Gorte et al. [13–19], possibly at the metal–support interface. This could involve activation of water at an oxygen vacancy on the surface of the zirconia adjacent to a Pt particle, followed by transfer of $O_{(ads)}$ to the Pt, where it could react with CO to release CO_2.

We emphasise that these considerations of possible reaction intermediates strictly apply only to this catalyst under these reaction conditions. Elsewhere [36,39,69], we have frequently emphasised the point that the *dominant* reaction mechanism for the WGS reaction is dependent on experimental parameters, such as the reaction temperature or the gas composition. To this we can now add the choice of support, because it seems abundantly clear that the mechanism on zirconia under these experimental conditions is different from that on ceria- or ceria/zirconia-supported catalysts. Finally, even for this catalyst, it must be stressed that the use of different experimental conditions (such as much higher water concentration, e.g., 52%, as used by Davis et al. [30], instead of the 7% used here) or a different metal or method of preparation of a zirconia-supported catalyst could result in different conclusions. The feed used in the present study also lacked the CO_2 that normally would be present in a true fuel processor. Some experiments with added CO_2 were carried out, but the analysis of the data was particularly complex because of the occurrence of the reverse reaction. It should be stressed that the dominant mechanism could change with increasing partial pressure of CO_2.

4. Conclusion

Only carbonyl and formate species were observed by in situ DRIFTS during the WGS reaction over our Pt/ZrO_2. The steady-state surface coverage of carbonate species was negligible. Isotopic transient kinetic analyses revealed that formates exchanged uniformly according to a first-order law, suggesting that most formates observed by DRIFTS were of the same reactivity. In addition, the time scale of the exchange of the reaction product CO_2 was significantly shorter than that of the surface formates. Therefore, the formate route, which is based on the formates seen on DRIFTS, can be ruled out as being the main reaction pathway in the present case. The number of precursors of the reaction product, CO_2, was lower than the number of surface Pt atoms, suggesting that carbonyl species, or some "infrared-invisible" complex (not excluding formates) at the interface between Pt and zirconia was the main reaction intermediate. A simple redox mechanism could also explain the present results.

Acknowledgments

The authors thank MEL for providing the ZrO_2 sample and Dr. Tiziano Montini, University of Trieste for performing the chemisorption measurements. Financial support was provided by MIUR (Italy) under the PRIN projects (to A.T.), the Carmac EPSRC project, and the CONCORDE Coordination Action on Nanostructured Oxides (NMP2-CT-2004-505834).

References

[1] C. Rhodes, G.J. Hutchings, A.M. Ward, Catal. Today 23 (1995) 43.
[2] M. Laniecki, M. Malecka-Grycz, F. Domka, Appl. Catal. A Gen. 196 (2000) 293.
[3] A.N. Fatsikostas, D.I. Kondarides, X.E. Verykios, Catal. Today 75 (2002) 145.
[4] K.A. Adamson, Energy Policy 32 (2004) 1231.
[5] C.C. Elam, C.E.G. Padro, G. Sandrock, A. Luzzi, P. Lindblad, E.F. Hagen, Int. J. Hydrogen Energy 28 (2003) 601.
[6] V. Idakiev, T. Tabakova, A. Naydenov, Z.-Y. Yuan, B.-L. Su, Appl. Catal. B Environ. 63 (2006) 178.
[7] W. Ruettinger, O. Ilinich, R.J. Farrauto, J. Power Sources 118 (2003) 61.
[8] R. Farrauto, S. Hwang, L. Shore, W. Ruettinger, J. Lampert, T. Giroux, Y. Liu, O. Ilinich, Ann. Rev. Mater. Res. 33 (2003) 1.
[9] P.S. Querino, J.R.C. Bispo, M.D. Rangel, Catal. Today 107–108 (2005) 920.
[10] H. Iida, A. Igarashi, Appl. Catal. A Gen. 303 (2006) 48.
[11] D. Tibiletti, A. Amieiro-Fonseca, R. Burch, Y. Chen, J.M. Fisher, A. Goguet, C. Hardacre, P. Hu, A. Thompsett, J. Phys. Chem. B 109 (47) (2005) 22553.
[12] S. Ricote, G. Jacobs, M. Milling, Y. Ji, P.M. Patterson, B.H. Davis, Appl. Catal. A Gen. 303 (2006) 35.
[13] W. Liu, M. Flytzani-Stephanopoulos, J. Catal. 153 (1995) 317.
[14] Q. Fu, H. Saltsburg, M. Flytzani-Stephanopoulos, Science 301 (2003) 935.
[15] Y. Li, Q. Fu, M. Flytzani-Stephanopoulos, Appl. Catal. B Environ. 27 (2000) 179.
[16] T. Bunluesin, R.J. Gorte, G.W. Graham, Appl. Catal. B Environ. 15 (1998) 107.
[17] R.J. Gorte, S. Zhao, Catal. Today 104 (2005) 18.
[18] S. Hilaire, S. Sharma, R.J. Gorte, J.M. Vohs, H.-W. Jen, Catal. Lett. 70 (2000) 131.
[19] S. Hilaire, X. Wang, T. Luo, R.J. Gorte, J. Wagner, Appl. Catal. A Gen. 215 (2001) 271.
[20] C.M.Y. Yeung, F. Meunier, R. Burch, D. Thompsett, S.C. Tsang, J. Phys. Chem. B 110 (2006) 8540.
[21] D.C. Grenoble, M.M. Estadt, D.F. Ollis, J. Catal. 67 (1981) 90.
[22] A. Luengnaruemitchai, S. Osuwan, E. Gulari, Catal. Commun. 4 (2003) 215.
[23] A. Venugopal, J. Aluha, M.S. Scurrell, Catal. Lett. 90 (2003) 1.
[24] S.L. Swartz, M.M. Seabaugh, C.T. Holt, W. Dawson, Fuel Cells Bull. 30 (2000) 7.
[25] T. Shido, Y. Iwasawa, J. Catal. 141 (1993) 71.
[26] G. Jacobs, L. Williams, U. Graham, G.A. Thomas, D.E. Sparks, B.H. Davis, Appl. Catal. A Gen. 252 (2003) 107.
[27] G. Jacobs, L. Williams, U. Graham, D. Sparks, B.H. Davis, J. Phys. Chem. B 107 (2003) 10398.
[28] G. Jacobs, U.M. Graham, E. Chenu, P.M. Patterson, A. Dozier, B.H. Davis, J. Catal. 229 (2005) 499.
[29] H. Iida, A. Igarashi, Appl. Catal. A Gen. 303 (2006) 48.
[30] E. Chenu, G. Jacobs, A.C. Crawford, R.A. Keogh, P.M. Patterson, D.E. Sparks, B.H. Davis, Appl. Catal. B Environ. 59 (2005) 45.
[31] G. Jacobs, E. Chenu, P.M. Patterson, L. Williams, D. Sparks, G. Thomas, B.H. Davis, Appl. Catal. A Gen. 258 (2004) 203.
[32] G. Jacobs, P.M. Patterson, L. Williams, E. Chenu, D. Sparks, G. Thomas, B.H. Davis, Appl. Catal. A Gen. 262 (2004) 177.
[33] G. Jacobs, P.M. Patterson, L. Williams, D. Sparks, B.H. Davis, Catal. Lett. 96 (2004) 97.
[34] M. Weibel, F. Garin, P. Bernhardt, G. Maire, M. Prigent, in: Catalysis and Automotive Pollution Control II, vol. 71, Elsevier, Amsterdam, 1991, p. 195.
[35] R.A. Koeppel, A. Baiker, C. Schild, A. Wokaun, J. Chem. Soc. Faraday Trans. I 87 (1991) 2821.
[36] D. Tibiletti, A. Goguet, F.C. Meunier, J.P. Breen, R. Burch, Chem. Commun. (2004) 1636.
[37] X.Q. Gong, P. Hu, R. Raval, J. Chem. Phys. 119 (2003) 6324.

[38] X.S. Liu, W. Ruettinger, X.M. Xu, R. Farrauto, Appl. Catal. B Environ. 56 (2005) 69.
[39] A. Goguet, F.C. Meunier, D. Tibiletti, J.P. Breen, R. Burch, J. Phys. Chem. B 108 (2004) 20240.
[40] F.C. Meunier, D. Tibiletti, A. Goguet, D. Reid, R. Burch, Appl. Catal. A Gen. 289 (2005) 104.
[41] E. Aneggi, J. Llorca, M. Boaro, A. Trovarelli, J. Catal. 234 (2005) 88.
[42] Z.-Y. Ma, C. Yang, W. Wei, W.-H. Li, Y.-H. Sun, J. Mol. Catal A Chem. 227 (2005) 119.
[43] D. Tibiletti, Ph.D. thesis, School of Chemistry, Queen's University Belfast (2004).
[44] M.W. Balakos, S.S.C. Chuang, G. Srivinas, J. Catal. 140 (1993) 281.
[45] J.M. Olinger, P.R. Griffiths, Anal. Chem. 60 (1988) 2427.
[46] D. Tibiletti, A. Goguet, D. Reid, F.C. Meunier, R. Burch, Catal. Today 113 (2006) 94.
[47] G. Busca, J. Lamotte, J.C. Lavalley, V. Lorenzelli, J. Am. Chem. Soc. 109 (1987) 5197.
[48] P. Bazin, O. Saur, J.C. Lavalley, M. Daturi, G. Blanchard, Phys. Chem. Chem. Phys. 7 (2005) 187.
[49] A. Holmgren, B. Andersson, D. Duprez, Appl. Catal. B Environ. 22 (1999) 215.
[50] A. Trovarelli, Catal. Rev. Sci. Eng. 38 (1996) 439.
[51] C. Binet, M. Daturi, J.C. Lavalley, Catal. Today 50 (1999) 207.
[52] C. Li, Y. Sakata, T. Arai, K. Domen, K. Maruya, T. Onishi, J. Chem. Soc. Faraday Trans. I 85 (1989) 929.
[53] N.B. Colthup, L.H. Daly, S.E. Wiberley, Introduction to Infrared and Raman Spectroscopy, Academic Press, Boston, 2000.
[54] K. Nakamoto, Infrared and Raman Spectra of Inorganic and Coordination Compounds, Wiley–Interscience, New York, 1986.
[55] S.L. Shannon, J.G. Goodwin, Chem. Rev. 95 (1995) 677.
[56] C.N. Costa, A.M. Efstathiou, J. Phys. Chem. B 108 (2004) 2620.
[57] Y. Schuurman, C. Mirodatos, Appl. Catal. A Gen. 151 (1997) 305.
[58] G. Jacobs, S. Ricote, U.M. Graham, P.M. Patterson, B.H. Davis, Catal. Today 106 (2005) 259.
[59] J. Crank, The Mathematics of Diffusion, second ed., Clarendon Press, Oxford, 1975.
[60] G. Muller, T. Narbeshuber, G. Mirth, J.A. Lercher, J. Phys. Chem. 98 (1994) 7436.
[61] F.C. Meunier, L. Domokos, K. Seshan, J.A. Lercher, J. Catal. 211 (2002) 366.
[62] E. Guglielminotti, Langmuir 6 (1990) 1455.
[63] C. Morterra, E. Giamello, L. Osio, M. Volante, J. Phys. Chem. 94 (1990) 3111.
[64] N.B. Jackson, J.G. Ekerdt, J. Catal. 101 (1986) 90.
[65] R.G. Silver, C.J. Hou, J.G. Ekerdt, J. Catal. 118 (1989) 400.
[66] J.C. Frost, Nature 334 (1988) 577.
[67] N.O. Gonzales, A.K. Chakraborty, A.T. Bell, J. Phys. Chem. B 101 (1997) 10058.
[68] M.D. Rhodes, A.T. Bell, J. Catal. 233 (2005) 198.
[69] R. Burch, Phys. Chem. Chem. Phys., invited article, in preparation.